Origin of solar systems: Organization

Lecture (KJ):

Introduction and overview
Dense molecular clouds, photo-dissociation regions and protostars

Protoplanetary disks
Equilibrium condensation of a solar nebula

Meteorites and the early solar system

Origin of giant planets

Comets and the early solar system

Student talks:

Origin of the elements and Standard Abundance Distribution

Agglomeration of planetesimals and protoplanets

Isotope chronology of meteorites and oxygen isotopes

Extrasolar planets

Transneptunian Objects

Protoplanetary disks

Protoplanetary disk:

Infall stage

Gas and Dust

Duration of infall stage comparable to free-fall collapse time of the core ~10^5-10^6 yr.
Matter with low specific angular momentum falls into the central star.
Matter with high specific angular momentum cannot reach the central star and forms the disk.

Parcel of gas falling from infinity to a circular orbit at heliocentric distance r_{SUN}.
Half of gravitational energy is converted to orbital kinetic energy, the other half per unit mass, is available for heat.
At 1 AU and 1 solar mass v_c = 30 km s^{-1} and the temperature in a hydrogen gas ~7 x 10^4 K, too high.

$$\frac{GM_{protostar}}{2r_{\odot}} = \frac{v_c^2}{2}$$

Two clouds meet from both sides of the forming disk, shock fronts form with temperatures ~1500 K at 1 AU and ~100 K at 10 AU.

Pressure in vertical direction:

$$P_z = P_{z_o} e^{-z^2/H_z^2},$$

Gaussian scale height Hz:

$$H_z = \sqrt{\frac{2kTr_{\odot}^3}{\mu_a m_{amu} G M_{\odot}}}.$$

It increases with distance: Tapered disk.

Internal dynamical evolution of the disk:

Redistribution of angular momentum can provide additional mass to the central star.
Magnetic torque can reduce rotation of star if ionization is high (frozen-in magn. field).

Protoplanetary disks apparently do not extend all the way down to the surface of the star. Magnetic interactions at the corotation point funnel some of the disk's gas onto the star and expel other gas in rapid centrifugally driven bipolar outflow which carries with it a substantial amount of angular momentum (?).

Gravitational torques: Nonaxisymmetric local instabilities can create spiral density waves like in galaxies or in the Saturnian ring system which limit the allowed mass of the disk.
Large protoplanets may clear annual gaps surrounding their orbits, excite density waves transporting angular momentum outwards. Similar effects can arise if protostar rotates sufficiently rapidly to become triaxial.

Internal dynamical evolution of the disk (continued):

Viscous torques: Molecules move on Keplerian orbits, i. e. its transverse speed decreases outwards. Collisions transfer mass inward and angular momentum outward (Lynden-Bell and Pringle).

Evolution on diffusion timescale: $t_d = \frac{\ell^2}{\nu_v}$, *l* = radius of the disk.

Viscosity largely unknown.

Molecular viscosity: $\nu_v \sim \ell_{fp} c_s$, l_{fp} mean free path of molecules and c_s sound speed.

Turbulent viscosity: $\nu_v = \frac{2}{3}\alpha_v c_s H_z$, $10^{-4} < \alpha_v < 10^{-2}$.

H_z depends on temperature and the disk temperature on opacity perp. to midplane. Well inside the orbit of Mercury the interstellar dust grains are all evaporated and opacity caused by H_2O and CO molecules and H ionization. At larger distances from the star the temperature is below 2000K and micrometer-sized dust is the dominant source of opacity.

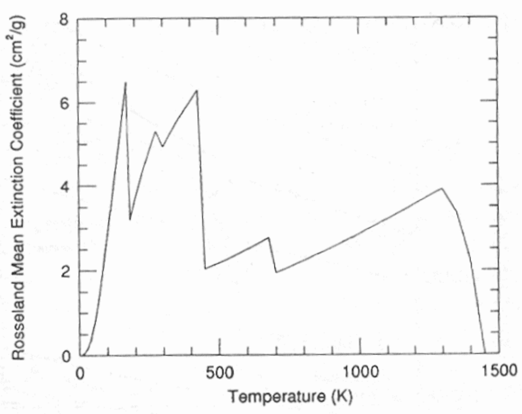

FIGURE 12.7 The Rosseland mean opacity of a solar composition mixture of gas and dust as a function of temperature. The size spectrum of the dust is assumed to resemble that of interstellar grains; the opacity is lower if the condensed material is contained in macroscopic bodies. The contribution of gas to the opacity is not included in these calculations, but at the low pressures occuring in protoplanetary disks, gas opacity is small compared to dust opacity at temperatures below 1400 K. (Adapted from Pollack *et al.* 1994)

Not derived because of lack of time:

Lynden-Bell D. and Pringle J.E. The evolution of viscous disks. MNRAS 168, 603-637, 1974.

Viscosity in a disk causes mass to drift inward and at the same time angular momentum to drift outward.

G. D'Angelo, T. Henning, and W. Kley
"Nested-grid calculations of disk-planet interaction"

A&A 385, 647-670

- Study of the evolution of an embedded protoplanet in a protostellar gas disk
- Nested grid to study simultaneously the global properties of the disk and the interaction of the planet with the disk
- Central star has one solar mass.
- Planetary mass ranges from M_{Earth} < MP < MJupiter
- Coordinate system rotates with the planet.
- Azimuth of planet $\varphi_P = \pi$

Equations:

Study surface density: $\Sigma = \int_{-\infty}^{\infty} \rho \mathrm{d}z$

Work in a coordinate system rotating with the planet: $\Omega = \Omega_\mathrm{p} = \sqrt{\frac{G(M_\star + M_\mathrm{p})}{a^3}}$,

2-dim (r,φ) continuity equation: $\frac{\partial \Sigma}{\partial t} + \nabla \cdot (\Sigma \boldsymbol{u}) = 0,$

$\omega = u_\varphi / r$, P is 2-dim pressure.

$$\frac{\partial(\Sigma u_r)}{\partial t} + \nabla \cdot (\Sigma u_r \boldsymbol{u}) = \Sigma r (\omega + \Omega)^2 - \frac{\partial P}{\partial r} - \Sigma \frac{\partial \Phi}{\partial r} + f_r$$

$$\frac{\partial[\Sigma r^2 (\omega + \Omega)]}{\partial t} + \nabla \cdot [\Sigma r^2 (\omega + \Omega) \boldsymbol{u}] = -\frac{\partial P}{\partial \varphi} - \Sigma \frac{\partial \Phi}{\partial \varphi} + f_\varphi$$

Gravitational potential: $\Phi = \Phi_\star + \Phi_\mathrm{p} = -\frac{G M_\star}{|\boldsymbol{r} - \boldsymbol{r}_\star|} - \frac{G M_\mathrm{p}}{|\boldsymbol{r} - \boldsymbol{r}_\mathrm{p}|}$

Pressure related to density Σ through $P = c_\mathrm{s}^2 \Sigma$

c_s sound speed, H scale height $c_\mathrm{s} = \frac{H}{r} v_\mathrm{Kep}$

v_{kep} Keplerian speed = $(GM_*/r)^{0.5}$

Constant h $h = \frac{H}{r} = 0.05$, i.e. $c_s = 0.05 * v_{Kep}$,

and *temperature = 70,000*0.05² = 175K for H gas* ($(mv^2/2) = kT$).

Viscosity:

Bulk viscosity ζ assumed =0.

Constant kinematic viscosity *ν*

$$f_r = \frac{1}{r}\frac{\partial(r S_{rr})}{\partial r} + \frac{1}{r}\frac{\partial S_{r\varphi}}{\partial \varphi} - \frac{S_{\varphi\varphi}}{r}$$

$$f_\varphi = \frac{1}{r}\frac{\partial(r^2 S_{r\varphi})}{\partial r} + \frac{\partial S_{\varphi\varphi}}{\partial \varphi}.$$

$$S_{rr} = 2\nu\Sigma\left(\frac{\partial u_r}{\partial r} - \frac{1}{3}\nabla\cdot\boldsymbol{u}\right),$$

$$S_{\varphi\varphi} = 2\nu\Sigma\left(\frac{\partial \omega}{\partial \varphi} + \frac{u_r}{r} - \frac{1}{3}\nabla\cdot\boldsymbol{u}\right)$$

$$S_{r\varphi} = \nu\Sigma\left(\frac{1}{r}\frac{\partial u_r}{\partial \varphi} + r\frac{\partial \omega}{\partial r}\right),$$

Divergence of velocity field: $\nabla \cdot \boldsymbol{u} = \frac{1}{r}\frac{\partial(r u_r)}{\partial r} + \frac{\partial \omega}{\partial \varphi}.$

H/r = 0.05 corresponds to a disk having mass influx rate ≈ 10^{-7} M_{Sun} yr^{-1}.
Kinematic viscosity coefficient α= 4×10^{-3} at the radial position r=1 of the planet $\nu = \alpha c_s H$
Total mass M_D of disk, extending from 2.08 to 13 AU = 3.5 x 10-3 M_{Sun}.
M_* = 1 M_{Sun} . the mass ratio $q = M_p/M_{sun}$ is the main variable parameter.

surface density, zooming in on the planet ..., M_P = 0.5 M_{Jup}

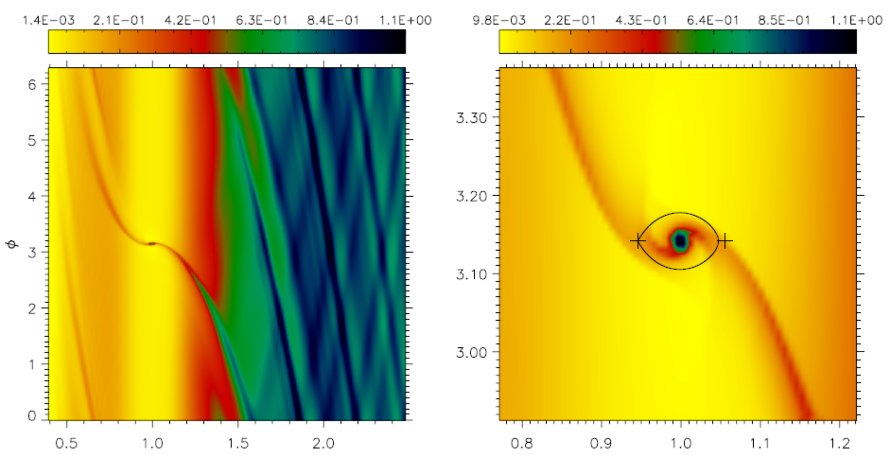

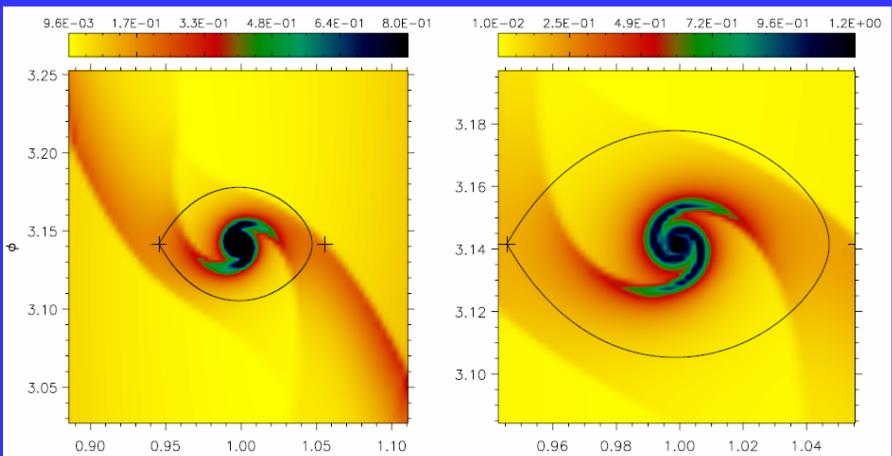

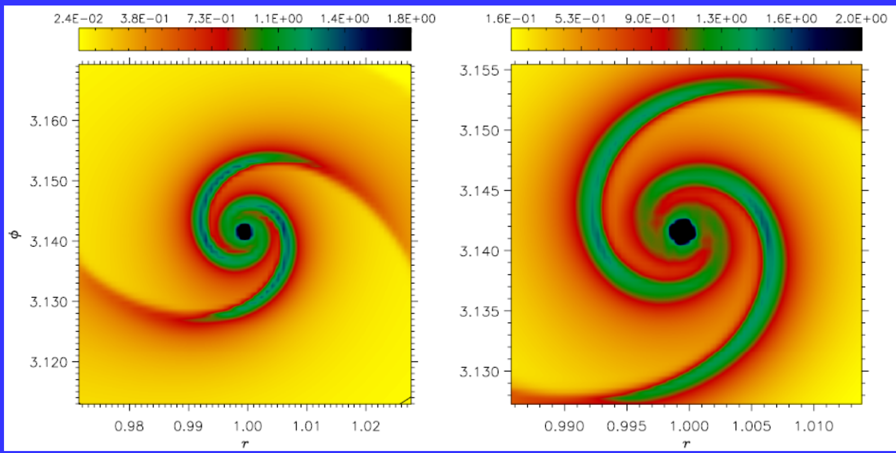

surface density and velocity vectors, $M_P = M_{Jup}$

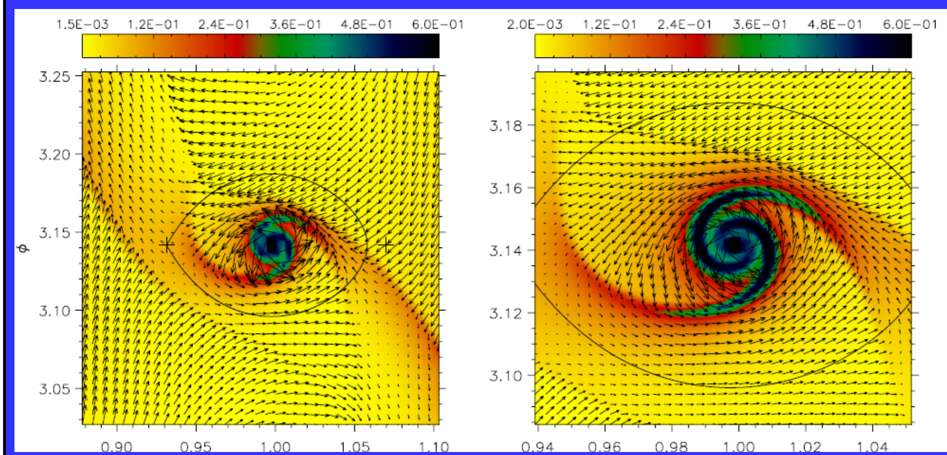

$M_P = 0.1\ M_{Jup}$

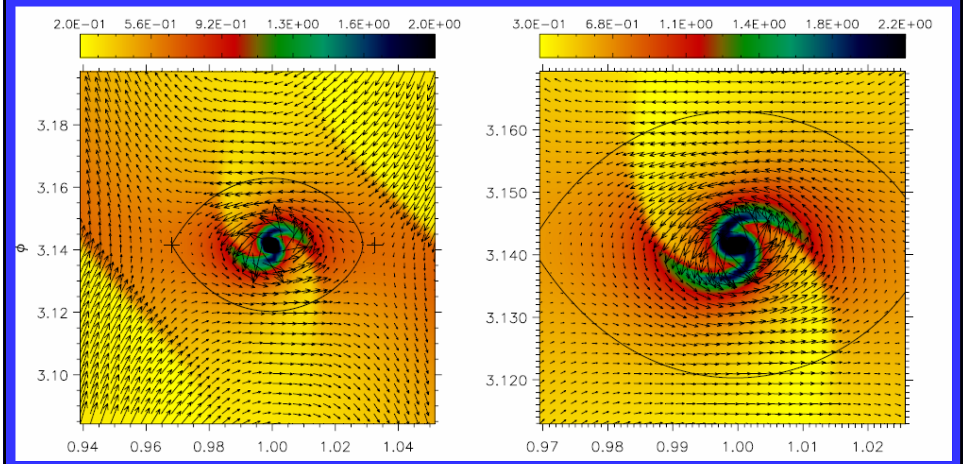

$M_P = 0.01\ M_{Jup}$

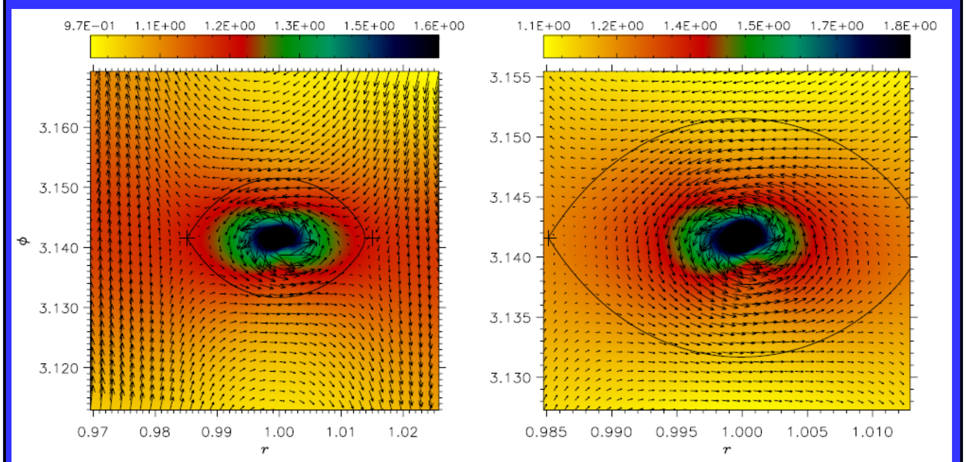

Torques exerted on the planet (note that part close to the planet is not considered)

low spatial resolution

high spatial resolution

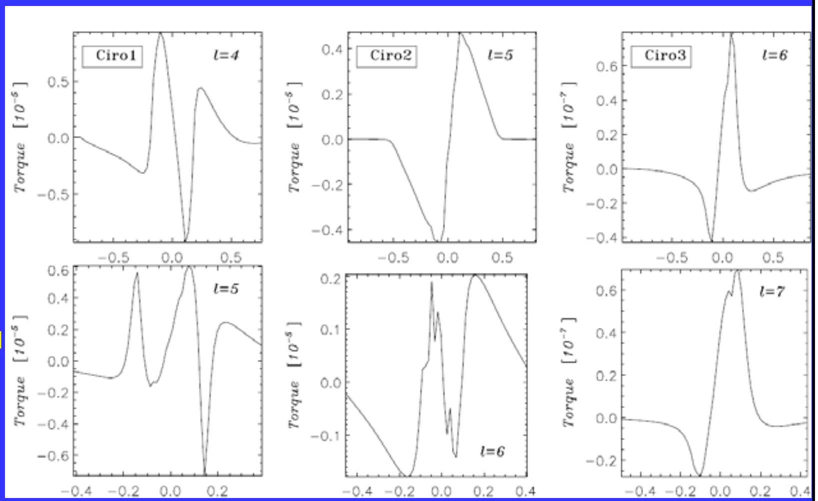

$M_P = M_{Jup}$ | $M_P = 0.1\ M_{Jup}$ | $M_P = 0.01\ M_{Jup}$

Note reversal of slope of torque for the large mass planet!

Inverse migration time scale versus M_P/M_{Sun} Planet at 5.12 AU in a disk with mass $M_D = 3.5 \times 10^{-3}\ M_*$.

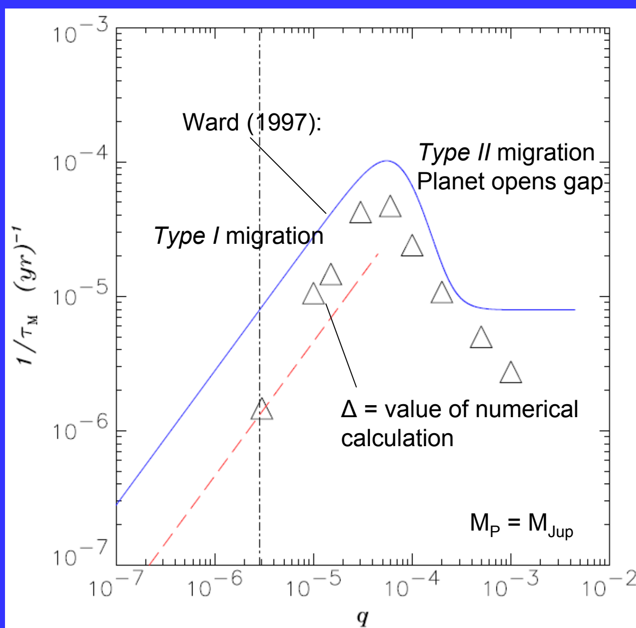

Ward (1997) type I migration:
a semi-major axis

$$\left(\frac{\mathrm{d}a}{\mathrm{d}t}\right)_{\mathrm{I}} \simeq -\frac{1}{2} q\, h^{-3}\, a\, \Omega_{\mathrm{p}} \left(\frac{\pi\, a^2\, \Sigma}{M_\star}\right)$$

Ward (1997) type II migration
Planet opens gap and the evolution is locked to the disk (viscous diffusivity).

$$\left(\frac{\mathrm{d}a}{\mathrm{d}t}\right)_{\mathrm{II}} = -\frac{3\,\nu}{2\,a} = -\frac{3}{2}\,\alpha\, h^2\, a\, \Omega_{\mathrm{p}}$$

Migration is always inward!

Equilibrium condensation of a solar nebula

Chemistry in the disk:

The initial chemical state of the disk depends upon the composition of the gas and dust in the interstellar medium and subsequent chemical processing during the collapse phase.

Comets and chondritic meterorites are relics from the planetesimal-forming era of the solar system's protoplanetary disk.

The composition of the Sun and the carbonaceous chondrites (unprocessed meterorites) tells us what the original elemental composition of the disk was, but not the chemical compounds these elements formed.

The chemical evolution of interstellar matter as it is incorporated into planetesimals via the disk process is fundamental to our understanding of planet formation.

T > 2000K (near the protostar): chemical equilibrium.
When chemical reaction times become comparable to the cooling time chemistry becomes more complicated (*freeze-out temperature*).

Examples CO/CH_4 and N_2/NH_3.
CO and N_2 dominate the inner solar nebula while in the cold outer nebula CH_4 and NH_3 would be favored.

But there are N_2 and CO ices on Pluto and Triton.

Calculations of the thermodynamically stable forms of C, O and N at the time when icy condensates began to form at 5 AU. The mass accretion rate of the protoplanetary disk for these calculations is 10^{-7} Mo per year.

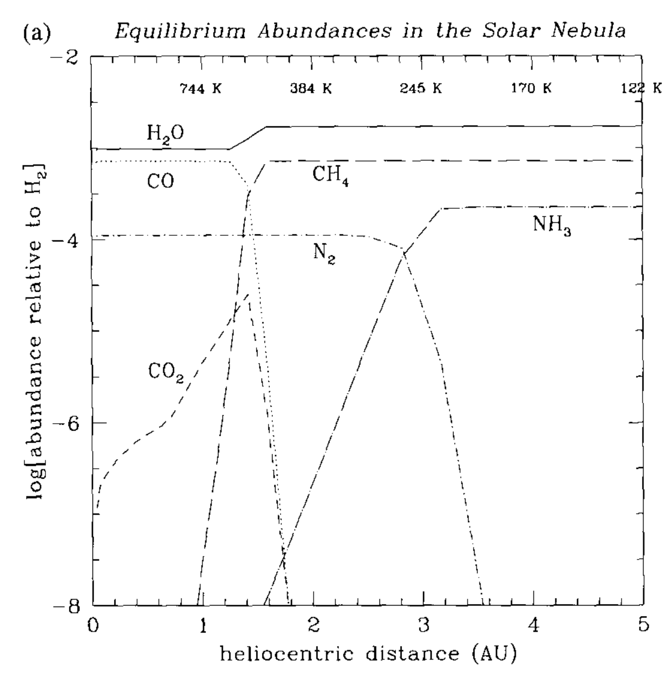

From chemistry textbook
(Hollemann-Wiberg: Lehrbuch der anorganischen Chemie, Berlin 1958):

Synthesis of ammonia gas (Haber-Bosch):
$3\ H_2 + N_2 \leftrightarrow 2\ NH_3 + 22.1$ kcal

a: exothermal → equilibrium shifts toward NH_3 if temperature gets lower.
at room temperature: equilibrium fully at the side of NH_3.
But reaction speed very low. Catalyst required.
b: volume shrinks → equilibrium shifts toward NH_3 if pressure gets higher.

Synthesis of gasoline (Fischer-Tropsch):
$n\ CO + (2n + 1)\ H_2 \leftrightarrow C_nH_{2n+2} + nH_2O$
$n\ CO + 2n\ H_2 \leftrightarrow C_nH_{2n} + nH_2O$

Note: CO and N_2 have the same electronic structure.

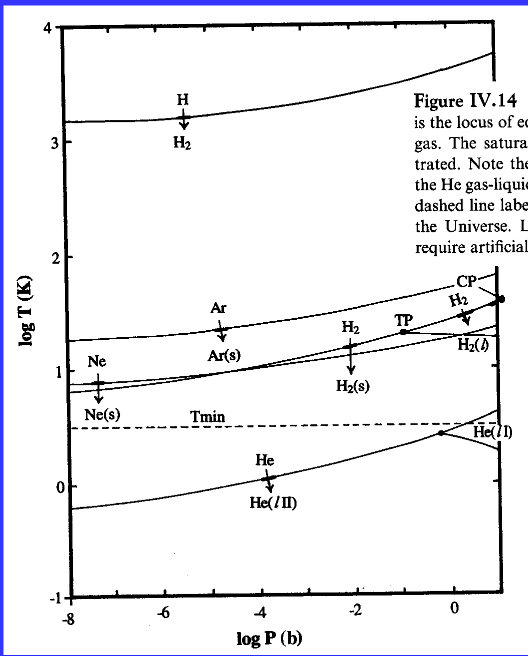

Figure IV.14 Hydrogen, helium, and neon chemistry. The top line is the locus of equal H and H_2 pressures: below it, H_2 is the dominant gas. The saturation temperatures for H_2, Ne, Ar, and He are illustrated. Note the triple point (TP) and critical point (CP) of H_2 and the He gas-liquid I–liquid II pseudo-triple point ("TP"). The horizontal dashed line labeled T_{min} is the microwave background temperature of the Universe. Lower temperatures, although not wholly impossible, require artificial (or natural) refrigeration.

This and the following slides from Lewis J.S.:
Physics and chemistry of the solar system, Chapter IV.
This chapter also treats the more refractory compounds (minerals).

1 bar = 0.987 atm

Cooling of an H–O–C–N mixture from about 3000 K gives rise to the following sequence of equilibrium reactions:

$$N + N \rightleftharpoons N_2 \tag{IV.99}$$

$$H + H \rightleftharpoons H_2 \tag{IV.100}$$

$$C + O \rightleftharpoons CO \tag{IV.101}$$

$$H + O \rightleftharpoons OH \tag{IV.102}$$

$$H + OH \rightleftharpoons H_2O \tag{IV.103}$$

$$CO + 3H_2 \rightleftharpoons CH_4 + H_2O \tag{IV.104}$$

$$N_2 + 3H_2 \rightleftharpoons 2NH_3 \tag{IV.105}$$

$$H_2O \rightleftharpoons H_2O(s) \tag{IV.106}$$

$$NH_3 + H_2O(s) \rightleftharpoons NH_3 \cdot H_2O(s) \tag{IV.107}$$

$$CH_4 + 7H_2O(s) \rightleftharpoons CH_4 \cdot 7H_2O(s) \tag{IV.108}$$

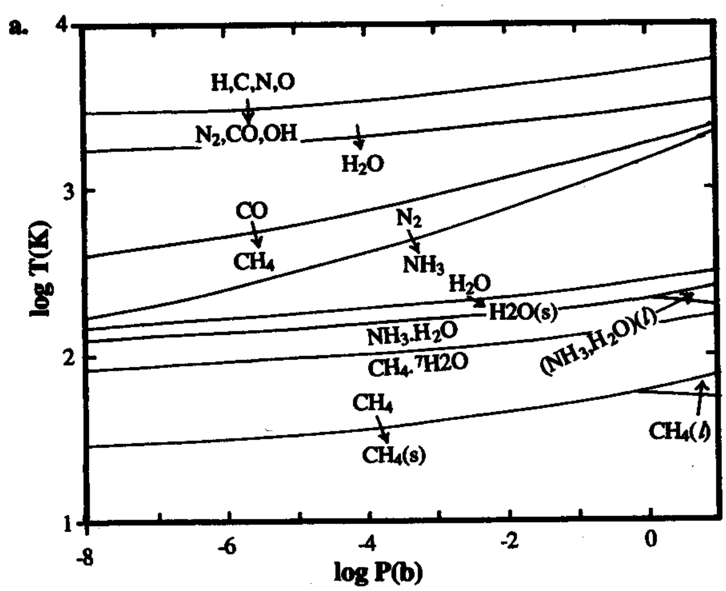

Figure IV.15 Carbon, nitrogen, and oxygen chemistry. Atomic H, C, N, and O combine to form OH, CO, and N_2 and thence stepwise to form H_2O, CH_4, and NH_3 as the temperature falls. The condensation processes are, in order, condensation of water ice I, partial conversion of ice I to ammonia monohydrate, conversion of all remaining water ice to the methane clathrate hydrate, and condensation of the leftover methane. b illustrates the equilibrium regions of dominance of the various compounds of C, N, and O. Note the region of thermodynamic stability of graphite at low pressures ($< 10^{-7}$ bar).

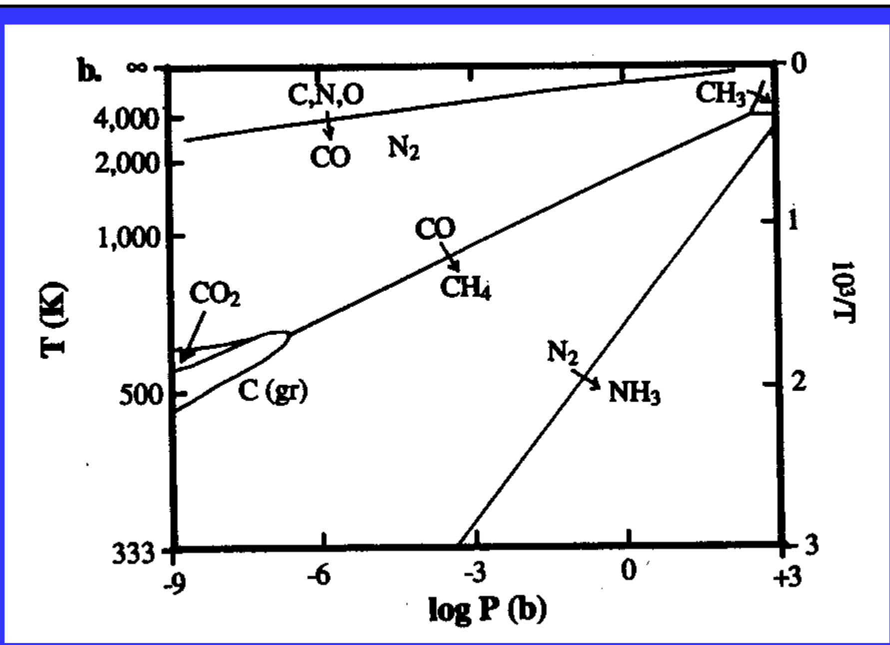

Higher pressure favors CH_4, NH_3, as said in the chemistry textbook!

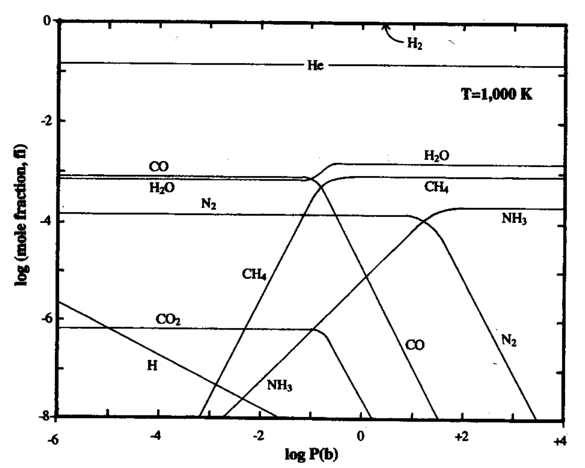

Figure IV.16 Mole fractions of H, C, N, and O gases along an isotherm. The crossover points for ammonia and methane at 1000 K are emphasized. Note also the CO_2 and H abundances.

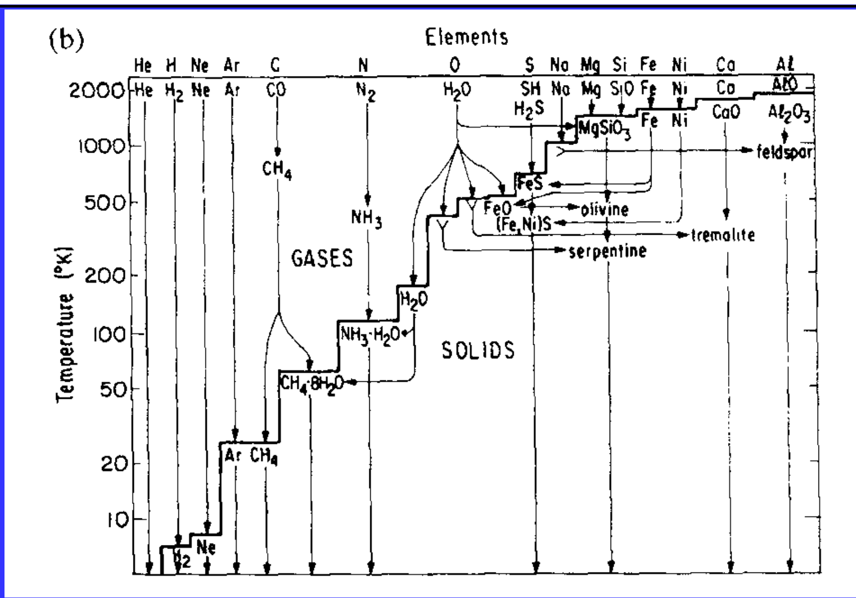

Flow chart of major reactions during fully equilibrated cooling of solar nebula material from 200 – 5 K. The 15 most abundant elements are listed across the top, and directly beneath the dominant gas species of each element at 2000 K (Barshay and Lewis 1976).

Thermochemical equilibrium stability fields for condensed material in a solar composition medium. The species diagrammed are in primarily solid form below the lines and primarily gaseous at higher temperatures. The dashed lines are estimated temperature-pressure profiles for the circumsolar and circumjovian disks (Prinn 1993).

Free parameter along dashed lines is *time*!

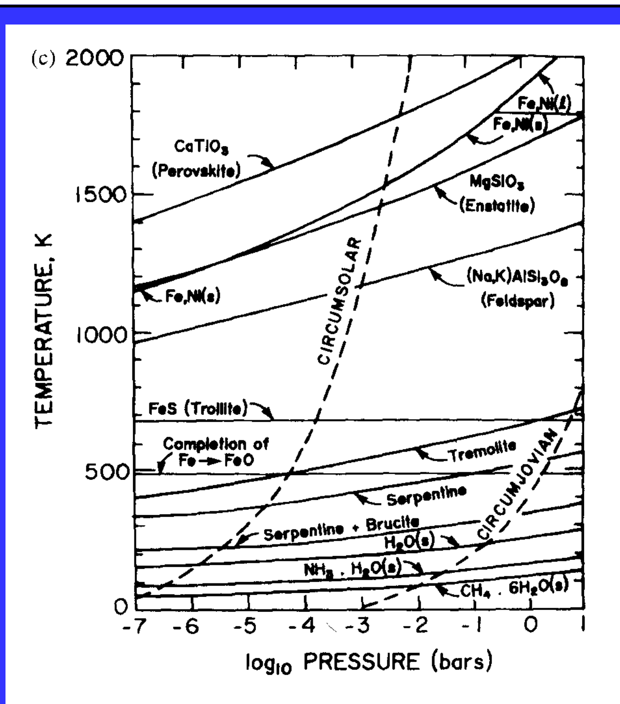

Role of stable CO in the condensation process (this and the next slide).

Here we see the solar system case (C/O = 0.43) where oxygen was more abundant than carbon, leaving the remaining O free to become bonded in into molecules which may condense into solids.

Whitted: “Dust in the galactic environment”, London 1992.

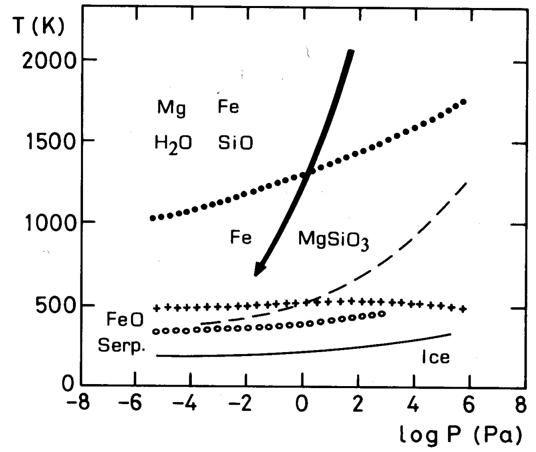

Figure 7.2 Temperature–pressure phase diagram illustrating stability zones of major solids in an atmosphere of solar composition (adapted from Salpeter 1974, 1977; Barshay and Lewis 1976). Above the dashed curve, gas phase CO is stable and essentially all C is locked up in this molecule. The most abundant gas phase reactants which lead to the production of solids are Fe, Mg, SiO and H_2O. The curved arrow indicates the variation in physical conditions which may occur in the outflow of a typical red giant. Magnesium silicates and solid Fe condense below the upper curve (• • •). At much lower temperatures, Fe is fully oxidized to FeO (below curve marked + + +) and may then be absorbed into silicates. Hydrous silicates such as serpentine are stable below the curve marked o o o. Finally, water-ice condenses below the continuous curve.

Case for C/O > 1.

Rings and PAHs may form via reactions

$C_2H_2 + H \rightarrow C_2H + H_2$

C_2H (C=CH) is ring segment.

$C_nH_m \rightarrow C_nH_{m-1} + H_2$
$C_nH_{m-1} + C_2H_2 \rightarrow C_{n+2}H_m + H$

PAH = polycyclic aromatic hydrocarbon

Whitted: “Dust in the galactic environment”, London 1992.

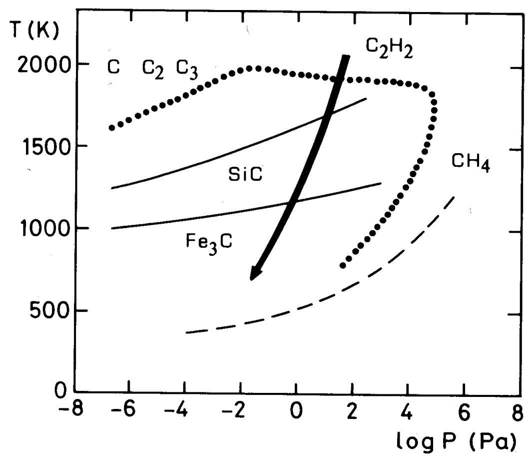

Figure 7.3 Temperature–pressure phase diagram illustrating stability zones of solids in a carbon-rich atmosphere (adapted from Salpeter 1974, 1977; Martin 1978). Solar abundances are assumed except that the abundance of C is enhanced to exceed that of O by 10%. Above the dashed line, gas phase CO is stable and essentially all O is locked up in this molecule. Other important gas phase carriers of C are labelled outside the dotted curve. The curved arrow indicates the change in physical conditions associated with a typical outflow from a red giant. Solid carbon is stable in the region enclosed by the dotted curve. Condensation curves for SiC and Fe_3C are also shown.

Non-equilibrium processes in the cold outer regions of the protoplanetary disk:

Low gas densities ~10^{-9} g cm^{-3}.
In interstellar medium 40% of carbon is in dust and 10% in PAHs, most gas-phase C is in CO.

Possibly CO and N_2 never converted to CH_4 and NH_3 in the cold outer regions.
NH_3 in cometary ices may be of interstellar origin.

End of chapter